ACS SENSORS

Article

Cite This: ACS Sens. XXXX, XXX, XXX−XXX

pubs.acs.org/acssensors

Peptide-Based Biosensing of Redox-Active Protein−Heme Complexes Indicates Novel Mechanism for Tumor Survival under Oxidative Stress

Kai Zhang,*[,†] Zhenqiang Fan,[†,§] Jiena Weng,[§] Jianfeng Zhao,[§] Jiaying Wang,[∥] Hao Wu,[†] Minhao Xie,[†] Hong Zhou,*[,⊥] and Hao Li*[,‡]

[†]Key Laboratory of Nuclear Medicine, Ministry of Health, Jiangsu Key Laboratory of Molecular Nuclear Medicine, Jiangsu Institute of Nuclear Medicine, Wuxi, Jiangsu 214063, China

[‡]School of Biological Science and Technology, University of Jinan, No. 106 Jiwei Road, Jinan, Shandong 250022, China

[§]Key Laboratory of Flexible Electronics (KLOFE) & Institute of Advanced Materials (IAM), Jiangsu National Synergetic Innovation Center for Advanced Materials (SICAM), Nanjing Tech University (NanjingTech), 30 South Puzhu Road, Nanjing 211816, China

[∥]Department of Rehabilitation & Acupuncture and Moxibustion, Nanjing Medical University, Affiliated Wuxi People's Hospital, Wuxi, Jiangsu 214000, China

[⊥]Key Laboratory of Optic-Electric Sensing and Analytical Chemistry for Life Science, Ministry of Education; Shandong Key Laboratory of Biochemical Analysis; Key Laboratory of Analytical Chemistry for Life Science in Universities of Shandong; College of Chemistry and Molecular Engineering, Qingdao University of Science and Technology, Qingdao 266042, China

Supporting Information

ABSTRACT: Signal response of several relevant protein−cofactor interactions, united in one bioassay, may greatly enhance the ability to study the intriguing molecular mechanisms of pathological process such as the tumor immunological process of chronic inflammation and oxidative stress. Here, a peptide-based multiplexed bioassay has been developed and applied in studying the interactions among ferritin, p53, and heme under oxidative stress. In a malignant breast cancer cell line, it can be observed that oxidative stress-triggered nuclear co-translocations of heme and ferritin may lead to direct molecular contact of ferritin with p53, to pass heme to p53, which subsequently sequestered into the cytoplasm, therefore forming a possible new route of tumor survival under oxidative stress, by using the stress to circumvent oxidative stress-induced apoptosis. The observed peroxidase-like activity of ferritin−heme and p53−heme complexes may also contribute to survival. Such activity is observed most prominently in triple negative or the most malignant breast cancer subtype. These results may suggest the possible future use of this bioassay in furthering the understanding of tumor molecular pathology, as well as the early detection, diagnosis, and prognosis of cancer.

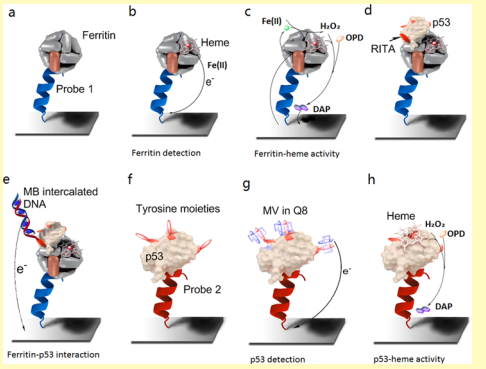

KEYWORDS: *protein−cofactor interactions, protein interaction, P53, tumor survival, oxidative stress, peptide-based biosensing, electrochemical biosensor*

Pathological development is an extremely complicated process involving large numbers of interconnected biofactors.[1−3] For example, cancerous conditions arise from chronic inflammation or prolonged local "oxidative stress".[4−8] This process is featured by numerous crosstalks among cellular and extracellular components of many different metabolic or immuno roles.[9−12] Trying to elucidate the molecular mechanisms behind such complex interplays, biomedical studies commonly employ conventional biomolecular methods such as western blotting, electrophoresis, etc. Such multi-procedure methods are usually time-consuming and labor-intensive, to the effect that it is often only practical for one research work to focus on one protein at a time, studying the interactions between no more than two relevant components. This situation greatly impairs the effort to obtain a comprehensive understanding of cancer molecular pathology. On the other hand, novel biosensing methods are often constructed in a simple assay form, in ready-to-be-used fashion.[13−16] The simplicity and multiplexity of these new biosensing methods may be promising in analyzing, in an integrated manner, the interactions and activities of several factors so that it might even become possible to shed light on a whole new pathway of cancer-related pathological reactions.

Received: June 12, 2019
Accepted: September 17, 2019
Published: September 17, 2019

DOI: 10.1021/acssensors.9b01083
ACS Sens. XXXX, XXX, XXX−XXX

Scheme 1. Proposed Method for Studying Ferritin−p53−Heme Interactions; Not Drawn to Scale

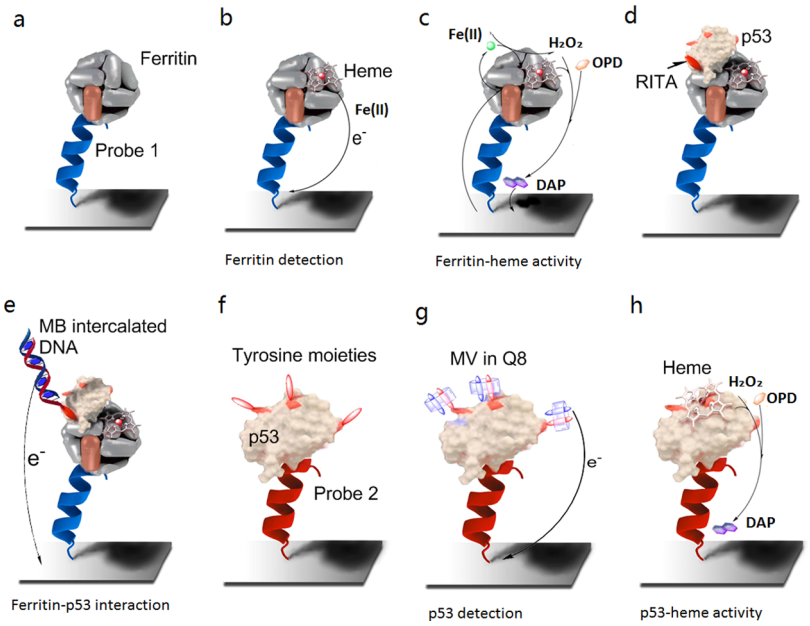

In this work, a possible pathway for tumor survival under oxidative stress is unveiled using a newly constructed multiplexed peptide-based bioassay, in observing the interactions between proteins and heme with varied redox activity. Oxidative stress is, epidemiologically, the cause of many cancers such as hepatocellular carcinoma.[17−20] However, the complicated and usually confusing interactions among proteins, metal ions, and other bioactive cofactors in oxidatively stressed conditions deny a clear-cut boundary between inflammatory condition and the early phase of cancerous development, thereby often nullifying the efforts of early detection and therapeutic intervention. On the other hand, it is currently believed that cancer can originate from prolonged local oxidative stress through the "screening" of cells: most cells end in apoptotic death due to oxidative stress-induced failure of stabilizing cellular redox potential, while the residual survivors who have successfully override this oxidative stress-induced apoptosis then become the progenitor of tumor colonies.[21−24] So, it may not be improper to postulate that there must be some interplay between factors respectively regulating oxidative stress and apoptosis. Indeed, previous reports can support this hypothesis, only that the evidence is circumstantial and often isolated. Here, using a newly designed peptide-based bioassay, the crosstalk between redox-regulating factors such as ferritin and heme, and apoptotic regulatory factor p53, can be observed. And it may be supposed that future early screen targeting this feature may not fail to discriminate early development toward cancerous growth from seemingly benign colonies of local inflammation.

This integrated bioanalysis of protein−cofactor interactions and activity is made possible by peptide but not the other type of recently developed artificial targeting ligand, namely, nucleic acid aptamer, because aptamer has limited availability of target proteins. When faced with several interconnected target proteins in an integrated analysis, it is more often than not that appropriate aptamers cannot be found for all of the target proteins. On the other hand, peptides derived from the same amino acids comprising proteins make peptides apt to mimic protein interactions. Meanwhile, peptides, like nucleic acids, have a simple and definite structure, enabling more versatile designs of low cost, compared to antibodies. Using this peptide-based assay, we can observe, in a tumor cell line, oxidative stress-induced nuclear co-translocation of ferritin and heme. Then, this nucleus-relocated ferritin, through direct contact with p53, transfers heme to p53. This results in p53−heme co-exportation from the nucleus. Through this mechanism, tumor cells employ oxidative stress to suppress the apoptotic activity of p53, facilitating their survival under hostile environment lethal to a normal cell, and may, at the same time, further their own cancerous phenotype. This discovery demonstrates the efficiency of the proposed peptide-based biosensing method in analyzing the interconnected activities of several proteins and biofactors, and this analysis, applied in clinical tissue samples, also shows the parallel between observed activity and the prognosis of cancer, indicating the feasibility of targeting such tumor survival mechanism as an effective way to detect early procancerous activity.

EXPERIMENTAL SECTION

Chemicals and Biological Materials. Peptide probe 1 for ferritin (HSNTYYFPKGGK[25]-11-Mercaptoundecanoic acid (MUA)) and probe 2 for p53 (YGRKKRRQRRR[26]-(MUA)) were custom-synthesized as lyophilized powder, purity > 95%, by Shanghai Science Peptide Co., Ltd. Recombinant p53 was from Novusbio; 5,5′-(2,5-furandiyl)bis-2-thiophenemethanol (RITA) from R&D system, equine spleen ferritin (multidomain macromolecule with an iron core, MV 440 kDa, as claimed and certified by the provider), MUA, 9-mercapto-1-nonanol (MN), methyl viologen (MV), cucurbit[8]uril (Q[8]), methylene blue (MB), and heme were from Sigma-Aldrich; and double-stranded DNA (5′ to 3′, GCGCGCGC, complementary stand: 5′ to 3′, GCGCGCGC, annealed together after heating to 80 °C) was from TaKaRa Biotechnology. All of the other chemicals were of analytical grade. The solutions of the peptide probe were prepared by dissolving the powder to 10 μM with 100 mM phosphate-buffered saline (PBS) (pH 7.4). The stock solution of heme (800 μM) was freshly prepared in dimethyl sulfoxide and stored in the dark. RITA was diluted to 2 μM with 100 mM PBS (pH 7.0). The MB-intercalated DNA label was prepared by incubating 10 μM annealed double-stranded DNA with 100 μM MB in 100 mM PBS (pH 7.0),

DOI: 10.1021/acssensors.9b01083
ACS Sens. XXXX, XXX, XXX−XXX

for 1 h and at room temperature, followed by dialysis against blank PBS to remove free MB. The host–guest MV-in-Q8 label in Scheme 1g was prepared as follows: Briefly, MV and Q8 powder of equal molar amounts were dissolved in 100 mM PBS (pH 7.0) to 750 μM, followed by moderate vortex agitating overnight. This solution was freshly prepared each time and was brought to its experimental application immediately subsequent to the agitation process. The originally buffered ferritin was 100 mM PBS (pH 7.0) to various desired concentrations as the standard samples. The original buffered p53 was dissolved with 100 mM PBS, pH 7.4 to the desired concentrations. All solutions were prepared with double-distilled water, which was purified with a Milli-Q purification system to a specific resistance of 18 MΩ cm. MDA-MB-231 (ATCC) was maintained in Leibovitz's L-15, 10% fetal bovine serum, and in a humidified atmosphere with no extra CO_2 at 37 °C. For the detection, the cells were treated with 0.5 mM H_2O_2 for 1 h[27] in 24-well culture plates (Nanjing Protein in Biotechnology Co.) at a density of 1×10^4 cells/cm^2. The cells were then collected, diluted (each sample contains roughly 1×10^5 cells), and fractioned using a nuclear extraction kit (Active motif). Both the nuclear and cytoplasmic samples were then used for detection. For the detection of clinical samples, serum samples were collected from patients of breast cancer and benign conditions at Nanjing Medical University Affiliated Wuxi People's Hospital after obtaining consent from the local ethics committee. The samples were from the primary lesion, the adjacent normal tissue, as well as from the liver metastatic site. The retrieved samples were immediately sliced on ice to 1 mm^3, followed by digestion with type II collagenase at 37 °C for 30 min. The resulted supernatant was centrifugated at 800 rpm for 5 min, and the pellet was resuspended with 100 mM PBS and fractioned with a nuclear fraction kit (Active motif) following the instruction of the manufacturer. The nuclear and cytoplasmic fractions were then used as the targets in the corresponding detections.

Electrode Treatment. Transparent Au slides (ITO slides ionsprit with roughly 100 Å Au layer) were cut to fit the size of the cuvette used for spectra measurement. These slides were cleaned by sonicating for 20 min in ethanolamine (20 wt %) at around 37 °C. After drying under mild stream of nitrogen, the slides were immersed in the assembly solution (2.5 μM probe 1 or probe 2 and 5 mM tris(2-carboxyethyl)phosphine hydrochloride (TCEP) in 10 mM PBS, pH 7.4) at 4 °C for 16 h, and TCEP was adopted to prevent disulfide formation between peptide probes. The slides were then immersed in 9-mercaptononanol (MN) solution (1 mM MN in 100 mM PBS, pH 7.4) at room temperature for 3 h.

Detection. By using standard samples to validate the proposed set of assays, the probe 1-modified slide was incubated with ferritin at 37 °C for appropriate time, and after gentle rinsing with ddH_2O and 5% Tween-20, electrochemical measurement of protein reduction or Fe-ion release was carried out (Scheme 1b). Alternatively, the slide was incubated in tandem with ferritin and 100 mM PBS (pH 7.0)-diluted heme (for 10 min) to study heme binding using fluorescence quenching or the peroxidase-like activity (Scheme 1d), which was measured as below: the slide was dipped in a 1 mM HCl solution (1 mL) containing 0.43 mg/mL *o*-phenylenediamine (OPD) for 1 min, and the obtained copper-ion containing solution was treated with boiling water for 15 min. The signal response of the generated DPA was then recorded using a freshly prepared bare gold electrode in the above reaction solution. For studying ferritin–p53 interaction, the probe 1-modified slide was incubated in sequence with standard samples of ferritin, p53, and the 1:1 mixture of RITA and MB-intercalated DNA label, before being brought to electrochemical measurement of MB response (Scheme 1e). The probe 2-modified slide was incubated first with p53 at 37 °C for proper time and then with 750 μM MV-in-Q8 label at room temperature for 30 min, followed by gentle rinsing with ddH_2O and 5% Tween-20 before electrochemical measurement (Scheme 1g). Alternatively, the slide, after incubation with p53, was further incubated with 100 mM PBS (pH 7.0)-diluted heme (for 10 min) to study heme binding using the peroxidase-like activity (Scheme 1h), which was measured similarly as above, but with 100 μM H_2O_2 added to facilitate the detection. The detection of cellular samples was similarly conducted, with the collected cytoplasmic and nuclear fractions evenly divided into five parts for the above set of five assays.

Experimental Measurements. Isothermal titration calorimetry (ITC) measurements were conducted using a MicroCal ITC200 System (GE Healthcare Life Sciences). The titration was conducted at 25 °C. The titration schedule consisted of 38 consecutive injections of 1 μL with at least a 120 s interval between injections. Heats of dilution, measured by titrating beyond saturation, were subtracted from each data set. All solutions were degassed prior to titration. The data were analyzed using Origin 7.0 software. Fluorescence emission spectra of surfaces were measured using a QM-4/2005 fluorescence spectrometer (Photon Technology International, Inc., Birmingham, NJ) equipped with a xenon lamp. This light source and the detector were in the same plane at right angle to each other. The slides were kept in a water-filled cuvette at 60° from the base of the cuvette for fluorescence measurements. The surface with the gold film was kept away from the light source and toward the detector. Activating peak wavelength for dityrosine is 325 nm, while that for 3,4-dihydroxyphenylalanine is around 360 nm. Surface plasma resonance (SPR) measurements were performed with an Autolab ESPRIT system (Echo Chemie B.V., the Netherlands) equipped with a 670 nm monochromatic p-polarized light resource. Electrochemical measurements were carried out on a CHI660E Potentiostat (CH Instruments) with a conventional three-electrode system: the modified electrode as the working electrode, a saturated calomel electrode (SCE) as the reference electrode, and a platinum wire as the counter electrode. Square-wave voltammograms were recorded in 100 mM PBS, pH 7.4, which was deoxygenated by purging with nitrogen gas and maintained under this inert atmosphere during the electrochemical measurements. The experimental parameters for EIS: bias potential, 0.224 V vs SCE; amplitude, 5 mV; frequency range, 0.1 Hz–10 kHz; electrolyte solution: 5 mM $Fe(CN)_6^{3-/4-}$ with 1 M KCl. The data are obtained from at least three times of independent experiments, and the error bars are shown in the figures.

RESULTS AND DISCUSSION

Peptide-based biosensing interfaces have first been designed for studying the interactions among ferritin, p53, and heme (Scheme 1). Ferritin-targeting peptide probes are immobilized on ITO slide (Scheme 1a) as the sensing surface for quantifying ferritin, studying ferritin–heme and ferritin–p53 interactions. The peptide probe targets the "pore" structures on the surface of ferritin,[25] which, after being captured by the probes, can be quantified electrochemically either by irreversible protein reduction[28] or by the reversible release of Fe(II) ion[29] (Scheme 1a). Heme binding with the surface-captured ferritin can be observed by accelerated release of Fe(II) ion promoted by heme[30] (Scheme 1b), or more sensitively by the peroxidase-like activity of ferritin–heme complex[31] (Scheme 1c), in which the heme promotes release of Fe(II) that may generate H_2O_2 through Fenton-like reactions, while the generated H_2O_2 can be consumed by heme-catalyzed oxidation of *o*-phenylenediamine (OPD) to electroactive 2,3-diaminophenazine (DAP); meanwhile, the released Fe(II) can be savaged by ferritin, back to its ferrous core. Binding of p53 to the captured ferritin can be examined using a p53-targeting small-molecule probe "RITA" (5,5′-(2,5-furandiyl)bis-2-thiophenemethanol) targeting the N-terminal transactivation domain[32,33] (Scheme 1d), away from the potential p53–ferritin binding site.[34] This probe can also promote protein-DNA cross-linking,[35] by this method using a methylene blue (MB)-intercalated double-stranded DNA, the ferritin-bound p53 can be labeled (Scheme 1e). On the other hand, using a peptide probe targeting the tetramerization domain of p53,[26] it can also be directly quantified and the

DOI: 10.1021/acssensors.9b01083
ACS Sens. XXXX, XXX, XXX–XXX

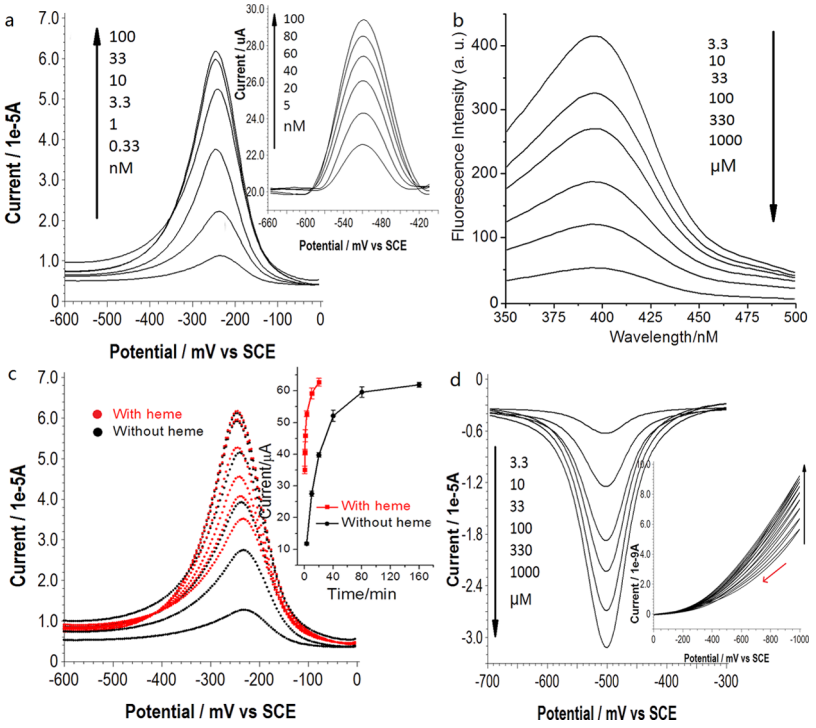

Figure 1. (a) Quantifying the ferritin captured by the surface-immobilized probe in Scheme 1a, using the released Fe(II) ion as signal readout; inset: quantification by ferritin reduction. (b) Quantification of gradually higher concentration of heme binding with 33 nM ferritin, by heme quenching the ferritin fluorescence. (c) Effect of heme binding to ferritin: acceleration of Fe(II) ion release, recorded by the peak response of Fe(II) released; inset: corresponding kinetic of Fe(II) ion release in the presence/absence of heme. (d) Effect of heme–ferritin interaction: peroxidase-like activity of ferritin–heme complex, recorded by gradually increased DAP production; inset: H_2O_2 evolution recorded during the process of catalytic DAP generation (the red arrow marks the direction of cyclic voltammetric scan).

heme–p53 interaction can be observed (Scheme 1f–h). In quantifying the binding of p53 with the peptide probes, methyl viologen (MV)-in-cucurbit[8]uril (Q8) host–guest label[36] is introduced to specifically mark the exposed tyrosine moieties on the surface of the captured p53 molecules (Scheme 1g); while the effect of heme binding with the captured p53 can be examined by the peroxidase-like activity[37,38] of p53–heme using OPD as the substrate in the presence of H_2O_2 (Scheme 1h).

Ferritin is a hollow protein shell enveloping a ferrous core, so ferritin molecules captured by the surface probes exhibit a peak around −0.55 V (vs Ag/AgCl), due to partial reduction of the outer protein shell[28] (Figure 1a inset), while more prominent signal readout can be observed around −0.2 V (Figure 1a) that may represent the release of Fe(II) ion.[29] Since every ferritin shell encloses hundreds of Fe atoms, this signal is much more sensitive than the reduction and is therefore chosen for the following applications. The interaction of ferritin with the targeting probe has also been investigated using isothermal calorimetry (ITC) method (Figure S1a), showing a typical sigmoid binding curve. The ferritin–probe interaction has also been optimized for the incubation time (Figure S2).

Ferritin–heme interaction is first investigated using standard ferritin and heme samples. The surface-captured standard ferritin is incubated with heme, and the characteristic 330 nm peak emission of ferritin (excited at 290 nm)[31] can be observed gradually quenched by gradually higher concentration of heme (Figure 1b). Meanwhile, the time course of Fe(II) release is greatly shortened by heme binding (Figure 1c),[30] pointing to possible consumption of the released Fe(II) by heme. By adding OPD as a substrate, oxidative conversion of OPD to DAP can be observed (Figure 1d), with observable evolution of H_2O_2 recorded (inset of Figure 1d), indicating possible peroxidase-like activity of the heme–ferritin complex as proposed above.[31] This catalytic method is also applicable to detect the potential formation of ferritin–heme complex in biological samples, while the observation of quenched ferritin fluorescence as well as the accelerated Fe(II) release must rely on standard heme-free ferritin as a control, so the catalytic activity is selected for detecting the ferritin–heme interaction in the following applications. The relatively weak ferritin–heme interaction can also be confirmed using the ITC method (Figure S1b).

Using an N-terminal targeting small-molecule probe,[31] standard p53 incubated with surface-captured standard ferritin is found to remain bound with ferritin,[34] as confirmed by the stepwise surface plasma resonance (SPR) sensorgram recorded upon the serial surface binding of ferritin, p53, RITA, and MB-intercalated DNA label (Figure 2a), supplemented by the gradual increase of MB electrochemical response by using p53 of gradually higher concentration (Figure 2b). This protocol of RITA recognition of p53 tandem p53-DNA cross-linking can also be employed for biological sample without standard proteins as the control. The interaction of moderate strength between p53 and ferritin can also be observed using ITC method (Figure S1c).

A second ITO sensing surface is modified with a peptide derived from HIV virus, targeting the tetramerization domain of p53,[26] away from the potential binding site of heme inside the core domain.[39] This peptide can capture p53 targets (peptide–p53 interaction as confirmed using the ITC method

DOI: 10.1021/acssensors.9b01083
ACS Sens. XXXX, XXX, XXX−XXX

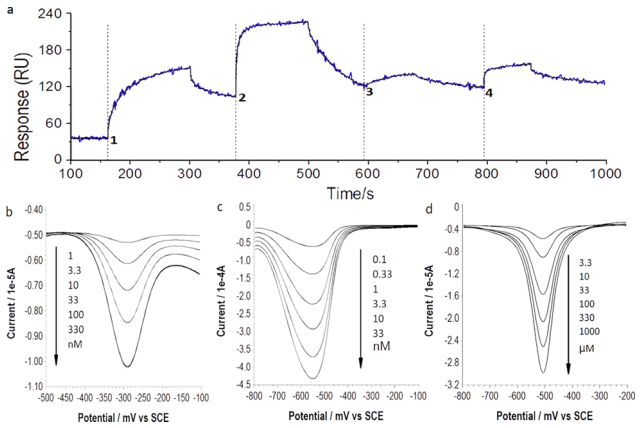

Figure 2. (a) Surface plasma resonance (SPR) sensorgram obtained by sequentially flowing (1) ferritin (3.3 nM), (2) p53 (33 nM), (3) RITA (1 μM), and (4) MB-intercalated DNA label across a gold slide modified by the ferritin-targeting probes. (b) Quantification of p53 binding with the surface-captured 3.3 nM ferritin, as illustrated in Scheme 1d,e, recorded as MB response. (c) Quantification of p53 captured by surface-immobilized probe shown in Scheme 1f, recorded as MV response. (d) Effect of heme−p53 interaction: peroxidase-like activity of ferritin−heme complex, recorded by gradually increased DAP production.

(Figure S1d), and the incubation time for the interaction has also been optimized (Figure S3)), and the captured p53 is labeled using a "host−guest" label of MV-in-Q8 as we have demonstrated previously,[36] yielding quantitative response with p53 concentration (Figure 2c), similar to the above quantitative result of ferritin detection.

Incubation of heme with the surface-captured p53 also results in peroxidase-like activity in the presence of added H_2O_2, in proportion to the concentration of heme used for incubation (Figure 2d), indicating p53 binding with heme to form a peroxidase-like complex. ITC data (Figure S1e) also support the presence of such a p53−heme interaction. The specificity of the ferritin and p53 probe have also been examined using various heme proteins as the control (Figure S4), and the specificity is found satisfactory.

Therefore, two peptide-modified biosensing interfaces have been constructed to examine five types of signal readout marking the complicated interplay among p53, ferritin, and heme (Scheme 1): the electroactivity of (1) released Fe(II) for ferritin detection, (2) DAP for ferritin−heme interaction, (3) MB for ferritin−p53 interaction, (4) Q8 for p53 detection, and again (5) DAP for ferritin−heme interaction, (1)−(3) on the surface bearing the ferritin-targeting probe while (4) and (5) with the p53-targeting probe-modified surface.

This method is then applied to detect ferritin−p53−heme interactions in MDA-MB-231, a malignant cell line of breast cancer,[40] subject to oxidative stress. In the absence of oxidative stress, as a parallel control, the above set of five simple assays are conducted (Figure 3a−e) in detecting, separately, the cytoplasmic and the nuclear samples. This procedure is repeated for the cells that have undergone the treatment (Figure 4a−e). The two sets of results are summarized, for clearance, in Table 1. It is clear that before oxidative stress, ferritin resides dominantly in the cytoplasm, but with only low level of peroxidase-like activity indicating heme−ferritin interactions, while p53 dominantly locates in the nucleus, without observable heme interaction. On the contrary after the stress, cytoplasmic ferritin is observed to decrease with a corresponding increase in the nuclear portion of the samples, both portions feature much more evident heme-induced peroxidase-like response; and p53 binding on the nuclear ferritin can be observed, for the first time. Meanwhile, compared to the situation in the absence of the stress, cytoplasmic p53 evidently increases with a corresponding moderate decrease in the nucleus. For both locations, heme-induced response with p53 is evident.

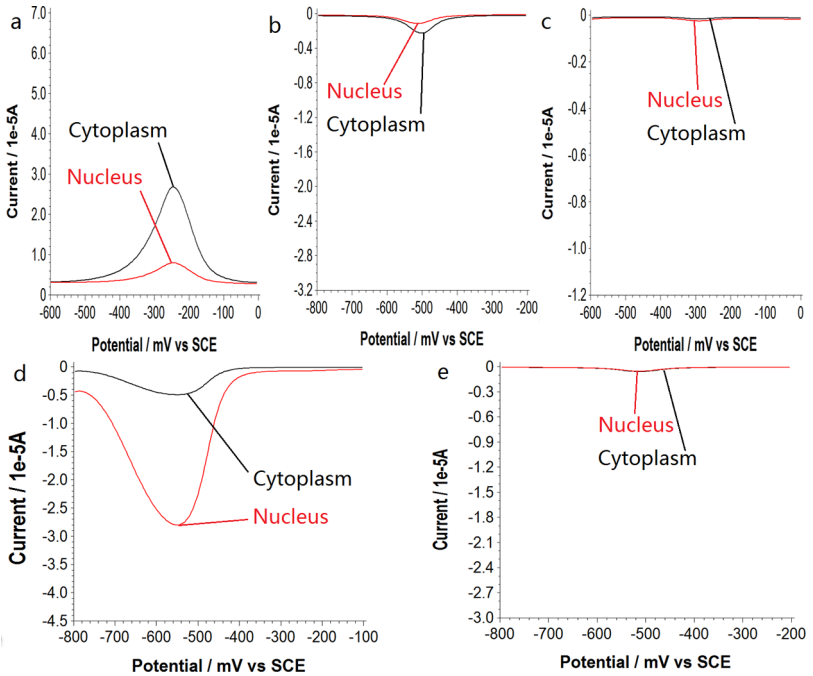

Figure 3. Detection of ferritin (a), ferritin−heme interaction (b), ferritin−p53 interaction (c), p53 (d), and p53−heme interaction, (e) in the cytoplasmic and nuclear fractions of MDA-MB-231 collected at 10^6 cells/mL, in the absence of oxidative stress.

DOI: 10.1021/acssensors.9b01083
ACS Sens. XXXX, XXX, XXX−XXX

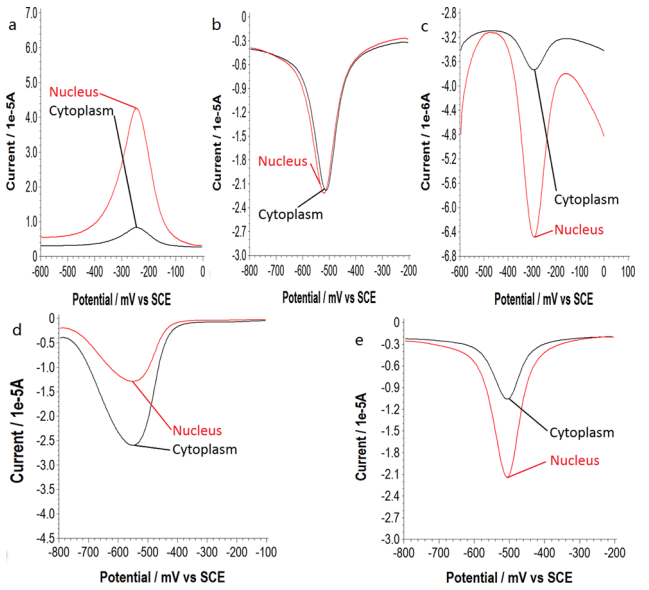

Figure 4. Detection of the above five aspects of ferritin−p53−heme interactions in fractions of MDA-MB-231 having undergone oxidative stress. Ferritin (a), ferritin−heme interaction (b), ferritin−p53 interaction (c), p53 (d), and p53−heme interaction (e) in the cytoplasmic and nuclear fractions of MDA-MB-231 collected at 10^6 cells/mL.

Table 1. Summary of the Cellular Results in Figures 3 and 4.

no oxidative stress	ferritin	ferritin−heme	ferritin−p53	p53	p53−heme
cytoplasm	√	low	×	×	×
nucleus	×	×	×	√	×
under oxidative stress	ferritin	ferritin−heme	ferritin−p53	p53	p53−heme
cytoplasm	low	√	low	√	√
nucleus	√	√	√	low	√

These results may allow a reconstruction of the following process triggered by the oxidative stress: the cytoplasmic ferritin first binds with free heme to initiate their co-translocation into the nucleus, where ferritin establishes direct molecular contact with p53,[34] the ferritin-bound heme molecules then redistribute, some of which may bind with p53 (both ferritin−heme and p53−heme interactions only have moderate binding strength comparable to each other, as we have examined above with ITC), and then, nuclear exportation of p53, with associated heme,[41] seems to initiate. This hypothesized process, derived from the above results, may benefit the survival of cancer cell under oxidative stress by both the ferritin nuclear importation and p53 nuclear exportation: ferritin is reported to protect the genome or chromosomes by relieving the strands of topological stress induced by oxidative cleavage and cross-linking of DNA,[42,43] while it is well known that p53's function is turned off by nuclear exportation and subsequent ubiquitin-induced digestion, and the function of p53 under oxidative stress is to initiate apoptotic gene transcription in the nucleus. Besides, the catalytic redox activity of both ferritin−heme and p53−heme[39,41] complexes, as we have observed here, may be connected with these subcellular translocations and antiapoptotic activities: the ferritin−heme complex, by its peroxidase activity, may be directly involved in the above-described nicking activity for genome protection; while the p53−heme complex may act as a scavenger of reactive oxygen species in the cytoplasm, and its gradual oxidative modification may finally dispose this complex to the ubiquitin-induced digestion. So, from our observation, in connection with previous reports, it seems oxidative stress may, in some types of cancer cells, induce a countermeasure involving components of both cellular redox potential regulation and apoptotic control, such as we have observed and proposed here that ferritin is recruited into the nucleus to protect the genome, while p53 is outcast from the nucleus to shut down the oxidative stress-induced apoptosis, and, interestingly, both processes are coordinated using heme. Such mechanisms may provide a tentative explanation as to the current controversy over the fluctuating and sometimes contradict effect of antioxidative therapy in many types of cancer.

Finally, detection of clinical tissue samples using the proposed method has also been attempted, using biopsy samples retrieved from breast cancer patients, and the set of the above five indicators show statistically significant difference between the cancerous and the paracancerous benign tissue (Figure 5a), while the heme-induced peroxidase-like activity of ferritin can be detected in nuclear portions of the samples, showing an agreement with prognostic grouping (Figure 5b): elevated ferritin peroxidase-like activity is strongly connected with triple-negative breast cancer, the most malignant subtype of breast cancer currently lacking any effective targeted therapy, consistent with previous literature report.[40]

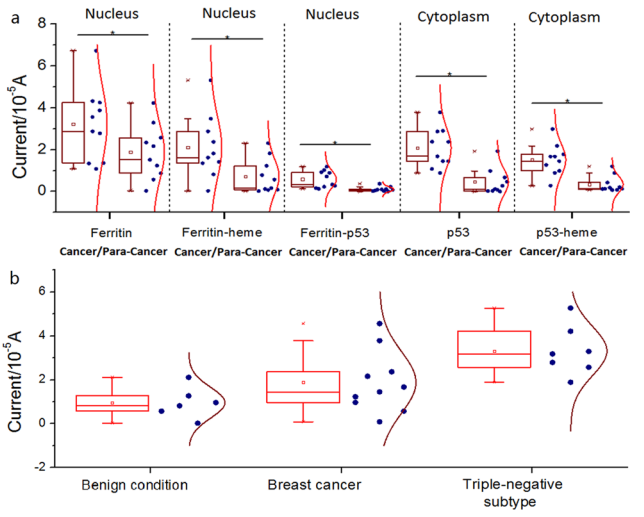

Figure 5. Box charts of the distribution of various detected signals in clinical biopsy samples. (a) The above five indexes as detected in the cancerous and paracancerous samples retrieved from victims of triple-negative breast cancer. (b) Nuclear ferritin−heme interaction detected in samples of different breast conditions.

CONCLUSIONS

We have here developed a peptide-based method to enable a set of simple assays to be readily applied in studying the interactions of several proteins and cofactors engaged in a particular pathological molecular mechanism. This strategy is demonstrated in studying the procancerous interactions among ferritin, p53, and heme. In a malignant cancer cell line, it can be observed that, under oxidative stress, cytoplasmic ferritin can bind with heme and co-translocate with it into the nucleus, where direct molecular contact with p53 takes place and p53

DOI: 10.1021/acssensors.9b01083
ACS Sens. XXXX, XXX, XXX−XXX

becomes heme-bound and in turn co-translocates with heme back to the cytoplasm. These observations taken together may support a hypothetic mechanism, among many currently proposed mechanisms, of tumor survival under oxidative stress, in which the tumor cells seem to manipulate the oxidative stress-induced events to counter the induced apoptosis. The interactions of ferritin and p53, with the heme cofactor, also result in peroxidase-like activity observed for the protein−heme complexes, and this type of activity is also supposed to be involved in the tumor survival mechanism. This activity is observed elevated in triple negative, or the most malignant type of breast cancer, suggesting a possible role of the proposed mechanism of surviving the procancerous oxidative stress in promoting cancer development. Using the proposed method to target such features involving multiple factors in cancer-promoting activity may also be a potential means for cancer early detection, diagnosis, and prognosis in the future.

■ ASSOCIATED CONTENT

Supporting Information

The Supporting Information is available free of charge on the ACS Publications website at DOI: 10.1021/acssensors.9b01083.

Isothermal titration calorimetry (ITC) titration, optimization of the incubation time for ferritin−probe peptide interaction; similar optimization of incubation time for p53−probe peptide interactions, and control experiments testing the specificity of the ferritin probe or other probes (PDF)

■ AUTHOR INFORMATION

Corresponding Authors

*E-mail: zhangkai@jsinm.org (K.Z.).
*E-mail: zhouhong@qust.edu.cn (H.Z.).
*E-mail: cardely@126.com. Tel: +86-510-85508775. Fax: +86-510-85508775 (H.L.).

ORCID

Kai Zhang: 0000-0002-7021-5395

Notes

The authors declare no competing financial interest.

■ ACKNOWLEDGMENTS

This work was supported by the National Natural Science Foundation of China (21705061, 810602737, 21675074, 81904055, and 21975126), the Natural Science Foundation of Jiangsu Province (BK20160991, BK20171470, and BK20171144), the Jiangsu Provincial Key Medical Discipline (Laboratory) (ZDXKA2016017), and the Innovation Capacity Development Plan of Jiangsu Province (BM2018023).

■ REFERENCES

(1) Chen, W.; Swanson, B. J.; Frankel, W. L. Molecular genetics of microsatellite-unstable colorectal cancer for pathologists. *Diagn. Pathol.* **2017**, *12*, No. 24.

(2) Ghidini, M.; Petrelli, F.; Hahne, J. C.; De Giorgi, A.; Toppo, L.; Pizzo, C.; Ratti, M.; Barni, S.; Passalacqua, R.; Tomasello, G. Clinical outcome and molecular characterization of brain metastases from esophageal and gastric cancer: a systematic review. *Med. Oncol.* **2017**, *34*, No. 62.

(3) Jin, K.; Li, T.; van Dam, H.; Zhou, F.; Zhang, L. Molecular insights into tumour metastasis: tracing the dominant events. *J. Pathol.* **2017**, *241*, 567−577.

(4) Kallens, V.; Tobar, N.; Molina, J.; Bidegain, A.; Smith, P. C.; Porras, O.; Martinez, J. Glucose Promotes a Pro-Oxidant and Pro-Inflammatory Stromal Microenvironment Which Favors Motile Properties in Breast Tumor Cells. *J. Cell. Biochem.* **2017**, *118*, 994−1002.

(5) Mitra, A.; Yan, J.; Xia, X.; Zhou, S.; Chen, J.; Mishra, L.; Li, S. IL6-mediated inflammatory loop reprograms normal to epithelial-mesenchymal transition(+) metastatic cancer stem cells in preneoplastic liver of transforming growth factor beta-deficient beta2-spectrin(+/-) mice. *Hepatology* **2017**, *65*, 1222−1236.

(6) Barajas-Gómez, B. A.; Rosas-Carrasco, O.; Morales-Rosales, S. L.; Pedraza Vazquez, G.; Gonzalez-Puertos, V. Y.; Juarez-Cedillo, T.; Garcia-Alvarez, J. A.; Lopez-Diazguerrero, N. E.; Damian-Matsumura, P.; Konigsberg, M.; Luna-Lopez, A. Relationship of inflammatory profile of elderly patients serum and senescence-associated secretory phenotype with human breast cancer cells proliferation: Role of IL6/IL8 ratio. *Cytokine* **2017**, *91*, 13−29.

(7) Harmon, B. E.; Wirth, M. D.; Boushey, C. J.; Wilkens, L. R.; Draluck, E.; Shivappa, N.; Steck, S. E.; Hofseth, L.; Haiman, C. A.; Le Marchand, L.; Hebert, J. R. The Dietary Inflammatory Index Is Associated with Colorectal Cancer Risk in the Multiethnic Cohort. *J. Nutr.* **2017**, *147*, 430−438.

(8) Merchant, J. L.; Ding, L. Hedgehog Signaling Links Chronic Inflammation to Gastric Cancer Precursor Lesions. *Cell. Mol. Gastroenterol. Hepatol.* **2017**, *3*, 201−210.

(9) Agliano, A.; Calvo, A.; Box, C. The challenge of targeting cancer stem cells to halt metastasis. *Semin. Cancer Biol.* **2017**, *44*, 25−42.

(10) Anderson, K. G.; Stromnes, I. M.; Greenberg, P. D. Obstacles Posed by the Tumor Microenvironment to T cell Activity: A Case for Synergistic Therapies. *Cancer Cell* **2017**, *31*, 311−325.

(11) Mangani, D.; Weller, M.; Roth, P. The network of immunosuppressive pathways in glioblastoma. *Biochem. Pharmacol.* **2017**, *130*, 1−9.

(12) Shaul, M. E.; Fridlender, Z. G. Neutrophils as active regulators of the immune system in the tumor microenvironment. *J. Leukoc. Biol.* **2017**, *102*, 343−349.

(13) Arugula, M. A.; Zhang, Y.; Simonian, A. L. Biosensors as 21st Century Technology for Detecting Genetically Modified Organisms in Food and Feed. *Anal. Chem.* **2014**, *86*, 119−129.

(14) Du, Y.; Dong, S. Nucleic Acid Biosensors: Recent Advances and Perspectives. *Anal. Chem.* **2017**, *89*, 189−215.

(15) Graybill, R. M.; Bailey, R. C. Emerging Biosensing Approaches for microRNA Analysis. *Anal. Chem.* **2016**, *88*, 431−450.

(16) Kimmel, D. W.; LeBlanc, G.; Meschievitz, M. E.; Cliffel, D. E. Electrochemical sensors and biosensors. *Anal. Chem.* **2012**, *84*, 685−707.

(17) Karimaian, A.; Majidinia, M.; Bannazadeh Baghi, H.; Yousefi, B. The crosstalk between Wnt/beta-catenin signaling pathway with DNA damage response and oxidative stress: Implications in cancer therapy. *DNA Repair* **2017**, *51*, 14−19.

(18) Martinez-Useros, J.; Li, W.; Cabeza-Morales, M.; Garcia-Foncillas, J. Oxidative Stress: A New Target for Pancreatic Cancer Prognosis and Treatment. *J. Clin. Med.* **2017**, *6*, No. 29.

(19) Prasad, S.; Gupta, S. C.; Tyagi, A. K. Reactive oxygen species (ROS) and cancer: Role of antioxidative nutraceuticals. *Cancer Lett.* **2017**, *387*, 95−105.

(20) Zhou, L.; Wen, J.; Huang, Z.; Nice, E. C.; Huang, C.; Zhang, H.; Li, Q. Redox proteomics screening cellular factors associated with oxidative stress in hepatocarcinogenesis. *Proteomics: Clin. Appl.* **2017**, *11*, 3−4.

(21) Saneesh Babu, P. S.; Manu, P. M.; Dhanya, T. J.; Tapas, P.; Meera, R. N.; Surendran, A.; Aneesh, K. A.; Vadakkancheril, S. J.; Ramaiah, D.; Nair, S. A.; Pillai, M. R. Bis(3,5-diiodo-2,4,6-trihydroxyphenyl)squaraine photodynamic therapy disrupts redox homeostasis and induce mitochondria-mediated apoptosis in human breast cancer cells. *Sci. Rep.* **2017**, *7*, No. 42126.

DOI: 10.1021/acssensors.9b01083
ACS Sens. XXXX, XXX, XXX−XXX

(22) Subash-Babu, P.; Alshammari, G. M.; Ignacimuthu, S.; Alshatwi, A. A. Epoxy clerodane diterpene inhibits MCF-7 human breast cancer cell growth by regulating the expression of the functional apoptotic genes Cdkn2A, Rb1, mdm2 and p53. *Biomed. Pharmacother.* **2017**, *87*, 388−396.
(23) Zeng, T.; Zhu, L.; Liao, M.; Zhuo, W.; Yang, S.; Wu, W.; Wang, D. Knockdown of PYCR1 inhibits cell proliferation and colony formation via cell cycle arrest and apoptosis in prostate cancer. *Med. Oncol.* **2017**, *34*, No. 27.
(24) Zheng, N.; Liu, L.; Liu, W. W.; Li, F.; Hayashi, T.; Tashiro, S. I.; Onodera, S.; Ikejima, T. Crosstalk of ROS/RNS and autophagy in silibinin-induced apoptosis of MCF-7 human breast cancer cells in vitro. *Acta Pharmacol. Sin.* **2017**, *38*, 277−289.
(25) Liu, X. S.; Patterson, L. D.; Miller, M. J.; Theil, E. C. Peptides selected for the protein nanocage pores change the rate of iron recovery from the ferritin mineral. *J. Biol. Chem.* **2007**, *282*, 31821−31825.
(26) Gabizon, R.; Mor, M.; Rosenberg, M. M.; Britan, L.; Hayouka, Z.; Kotler, M.; Shalev, D. E.; Friedler, A. Using peptides to study the interaction between the p53 tetramerization domain and HIV-1 Tat. *Biopolymers* **2008**, *90*, 105−116.
(27) Lesniak, W.; Szczepanska, A.; Kuznicki, J. Calcyclin (S100A6) expression is stimulated by agents evoking oxidative stress via the antioxidant response element. *Biochim. Biophys. Acta, Mol. Cell Res.* **2005**, *1744*, 29−37.
(28) Ritzert, N. L.; Casella, S. S.; Zapien, D. C. Surface-electrochemistry of ferritin adsorbed on 8-mercaptooctanoic acid-modified gold electrodes. *Electrochem. Commun.* **2009**, *11*, 827−830.
(29) Tominaga, M.; Ohira, A.; Yamaguchi, Y.; Kunitake, M. Electrochemical, AFM and QCM studies on ferritin immobilized onto a self-assembled monolayer-modified gold electrode. *J. Electroanal. Chem.* **2004**, *566*, 323−329.
(30) Kadir, F. H.; al-Massad, F. K.; Moore, G. R. Haem binding to horse spleen ferritin and its effect on the rate of iron release. *Biochem. J.* **1992**, *282*, 867−870.
(31) Jaafari, M.; Kooshk, M. R. A.; Asghari, S. M.; Moosavi-Movahedi, A. A.; Ghobadi, S.; Khodarahmi, R. Direct evidence for non-specific peroxidase activity of 'ferritin−heme" complex: possible role in the development of neurodegenerative diseases. *J. Iran. Chem. Soc.* **2015**, *12*, 779−790.
(32) Yu, X.; Narayanan, S.; Vazquez, A.; Carpizo, D. R. Small molecule compounds targeting the p53 pathway: are we finally making progress? *Apoptosis* **2014**, *19*, 1055−1068.
(33) Selivanova, G. Therapeutic targeting of p53 by small molecules. *Semin. Cancer Biol.* **2010**, *20*, 46−56.
(34) Lee, J. H.; Jang, H.; Cho, E. J.; Youn, H. D. Ferritin binds and activates p53 under oxidative stress. *Biochem. Biophys. Res. Commun.* **2009**, *389*, 399−404.
(35) Nieves-Neira, W.; Rivera, M. I.; Kohlhagen, G.; Hursey, M. L.; Pourquier, P.; Sausville, E. A.; Pommier, Y. DNA protein cross-links produced by NSC 652287, a novel thiophene derivative active against human renal cancer cells. *Mol. Pharmacol.* **1999**, *56*, 478−484.
(36) Li, H.; Xie, H.; Cao, Y.; Ding, X.; Yin, Y.; Li, G. A General Way to Assay Protein by Coupling Peptide with Signal Reporter via Supermolecule Formation. *Anal. Chem.* **2013**, *85*, 1047−1052.
(37) Moffet, D. A.; Certain, L. K.; Smith, A. J.; Kessel, A. J.; Beckwith, K. A.; Hecht, M. H. Peroxidase activity in heme proteins derived from a designed combinatorial library. *J. Am. Chem. Soc.* **2000**, *122*, 7612−7613.
(38) Obataya, I.; Kotaki, T.; Sakamoto, S.; Ueno, A.; Mihara, H. Design, synthesis and peroxidase-like activity of 3alpha-helix proteins covalently bound to heme. *Bioorg. Med. Chem. Lett.* **2000**, *10*, 2719−2722.
(39) Shen, J.; Sheng, X. P.; Chang, Z. N.; Wu, Q.; Wang, S.; Xuan, Z. L.; Li, D.; Wu, Y. L.; Shang, Y. J.; Kong, X. T.; Yu, L.; Li, L.; Ruan, K. C.; Hu, H. Y.; Huang, Y.; Hui, L. J.; Xie, D.; Wang, F. D.; Hu, R. G. Iron Metabolism Regulates p53 Signaling through Direct Heme-p53 Interaction and Modulation of p53 Localization, Stability, and Function. *Cell Rep.* **2014**, *7*, 180−193.
(40) Shpyleva, S. I.; Tryndyak, V. P.; Kovalchuk, O.; Starlard-Davenport, A.; Chekhun, V. F.; Beland, F. A.; Pogribny, I. P. Role of ferritin alterations in human breast cancer cells. *Breast Cancer Res. Treat.* **2011**, *126*, 63−71.
(41) Shen, J.; Sheng, X.; Chang, Z.; Wu, Q.; Xie, D.; Wang, F.; Hu, R. The heme-p53 interaction: Linking iron metabolism to p53 signaling and tumorigenesis. *Mol. Cell Oncol.* **2016**, *3*, No. e965642.
(42) Surguladze, N.; Thompson, K. M.; Beard, J. L.; Connor, J. R.; Fried, M. G. Interactions and reactions of ferritin with DNA. *J. Biol. Chem.* **2004**, *279*, 14694−14702.
(43) Alkhateeb, A. A.; Connor, J. R. Nuclear ferritin: A new role for ferritin in cell biology. *Biochim. Biophys. Acta, Gen. Subj.* **2010**, *1800*, 793−797.

DOI: 10.1021/acssensors.9b01083
ACS Sens. XXXX, XXX, XXX−XXX